1998 International Computer Symposium
Workshop on Computer Graphics and Virtual Reality
December 17-19, 1998, N.C.K.U., Tainan, Taiwan, R.O.C.

THE APPLICATION OF PHOTOMETRIC STEREO TO 3D FACIAL SURFACE MEASUREMENT

Kuo-sheng Cheng, Ja-ming Hu, and Yen-ting Chen

Institute of Biomedical Engineering
National Cheng Kung University, Tainan, Taiwan, R.O.C.
Email: kscheng@mail.bme.ncku.edu.tw

ABSTRACT

Computer graphics techniques have been extensively applied in the medical field, especially for three dimensional visualization and surgical simulation. In dental and plastic surgery, surface for the human face is only concerned. Computed tomography (CT) and magnetic resonance imaging (MRI) may not be appropriate modalities for use in 3D surface reconstruction. Photometric stereo method is a method with the advantages of fast, cheap, and simple. It is a technique to make use of the shading information to reconstruct shape from several images taken under different directions of incident illumination. In this research, a photometric stereo system is built and applied to measure the 3D shape of human face. From the experimental results, it is demonstrated that the human faces would be near lambertian with the help of the makeup used to remove the specularity. In addition, four images are obtained to recover the lost information in shadow areas. The near point light source model is also proposed for correction with an iterative scheme. Above all, it is shown the reconstruction accuracy of this system is better than the conventional Photometric stereo method.

1. INTRODUCTION

Computer graphics techniques have been extensively applied in the medical field, especially for three dimensional visualization and surgical simulation. These applications need accurate acquisition of three dimensional data usually provided by 3D imaging modalities, such as computed tomography (CT), magnetic resonance image (MRI). However, many medical image applications in dental and plastic surgery are only concerned with the surface shape of human faces. Therefore, these modalities are too expensive and might be considered "over-specifications" for these applications, in which the internal structure information of the bodies is not used.

In recent years, 3D digitizers or surface scanners have been developed and utilized for this purpose. Although they provide rather high resolution and accuracy of range data[1-3], the speed of scanning process is still not fast enough to avoid the errors due to subject movement. To overcome this problem, extra facilities are often needed so that the system becomes complicated and the expenses increases.

Photometric stereo method was firstly proposed by Woodham in 1980[4]. By making use of the shaded information, shape can be recovered from several images taken under the different directions of incident illumination with fixed viewing direction. In comparison with those techniques mentioned above, the advantages of photometric stereo are cheap and simple. There are no expensive facilities are required. The major components of the whole system are only light bulbs, a camera, a dark room and a personal computer. It is very easy to set up the system. These imply that the photometric stereo method has the great potential in the application to facial surface measurement.

In computer vision, researches on shape recovery from images have been conducted for more than two decades. Shape from shading (SFS) is to recover the shape from the variation of intensity on an image with the knowledge of direction of incident illumination. In 1980, Woodham[4] found that an unique solution can be directly determined using three images. In his method, the objects are illuminated by three different directions of light sources as the positions of the camera and the object are held unchanged. To be distinguished from conventional stereo vision, this technique is named Photometric Stereo (PMS) because it uses the radiance values recorded on the images rather than the displacement between corresponding points.

In this study, an photometric stereo system is set up to measure surface contours of human face. Different from the conventional PMS, four images under different illumination directions are used. In addition, near point source model is employed and the orientations of surface points are determined by using an iterative scheme.

The remainder of this paper is organized as follows. The basic principles underlying the system design are described in section two. In section three, our algorithm is described in detail. Section four is devoted to the experiments and their results. Finally, conclusions and future developments are given in section five.

2. PRINCIPLES AND SYSTEM DESIGN

2.1 The Reflectance Model

Images are the sets of intensity values which are the

records of radiance reflected from the illuminated objects. The reflected radiance depends on the physical properties and the shape of the object when the incident radiance has constant direction and intensity. According to their physical properties, surface can be categorized as pure lambertian, pure specular and hybrid.

If the surfaces are rough enough so that all incident light beams are diffusively reflected to all directions. These surfaces are so-called lambertian surfaces. Since the probability of reflection is the same for all directions, the observed brightness is the same no matter where the viewer stands. The intensity of reflection for the lambertian surface I_L can be modeled as the product of the strength of the light source I_i, the reflectance factor of the surface ρ, and the inner product of the surface normal N and light source direction L[5].

$$I_L = I_i \rho \vec{N} \cdot \vec{L} = I_i \rho \cos\theta \tag{1}$$

If the surface is smooth like a mirror, specularity occurs at the angle equal to that between incident light and the surface normal. Specularity consists of two components, specular lobe and specular spike. If the surface of an object is near lambertian, the specular components can be neglected. With a given light source, surface normal can be possibly found by calculating the reflectance map derived from Eq. (1).

2.2 Photometric Stereo Method

The basic idea of PMS is to solve Eq. (1) for the unknown surface normal. When three images in the same view are taken under different lighting directions, then three reflectance maps are provided for solving a linear system of three unknowns *nx, ny,* and *nz*.

Let the intensities of a point (x, y) recorded on three images be a column vector $\vec{I} = [I_1\ I_2\ I_3]^T$ and the directions of three light sources be $\vec{l}_1, \vec{l}_2, \vec{l}_3$, which are unit vectors and form the matrix L as follows.

$$\mathbf{L} = \begin{bmatrix} \vec{l}_1 & \vec{l}_2 & \vec{l}_3 \end{bmatrix}^T = \begin{bmatrix} l_{1x} & l_{1y} & l_{1z} \\ l_{2x} & l_{2y} & l_{2z} \\ l_{3x} & l_{3y} & l_{3z} \end{bmatrix} \tag{2}$$

Let $\vec{n} = [n_x\ \ n_y\ \ n_z]^T$ be the unit surface normal vector at (x, y). Then

$$\vec{I} = \rho\, \mathrm{L}\, \vec{n} \tag{3}$$

so we have $\rho \vec{n} = \mathrm{L}^{-1}\vec{I}$, provided that L is non-singular. Since $\vec{n}$ is unit length, we have

$$\begin{aligned} \| \rho\, \vec{n} \| &= \rho \| \vec{n} \| \\ &= \rho = \| \mathrm{L}^{-1}\vec{I} \| \end{aligned} \tag{4}$$

and

$$\vec{n} = \frac{1}{\rho} \mathrm{L}^{-1}\vec{I}, \tag{5}$$

Therefore, the normal vector is determined.

2.3 Light Source Arrangement

Spatial distribution

An important procedure in conventional PMS is to calculate the inverse illumination direction matrix. Therefore, this matrix should be non-singular. Moreover, it is also suggested that light source directions had better be as far as possible in order to reduce the error due to digitization of intensities.

In practical application, the range of available illumination direction is often restricted by its measurement environment. This implies that the light source directions need to be nearly collinear with the viewing direction. This may cause the illumination matrix to be ill-conditioned. To cope with this situation, singular value decomposition (SVD)[6] technique is employed to constrain how collinear the light source directions can be with one another.

Although the optimal solution for light source placement is varied with the measurement situation and the shape of the target object, the rule is always to obtain the larger weight of maximum difference of illumination directions and minimum shadow areas.

Near or far point source

PMS assume parallel incident light beams. To meet this requirement, the point sources need to be placed very far away from the object or the distance between the source and the object should be much larger than the dimension of the object.

When the ordinary light bulbs are used, the intensities of radiance will be seriously attenuated because the radiance of the incident illumination is a function of the squared distance. Therefore, the near point light source model is considered and incorporated into PMS to determine the real surface orientation. Iterative schemes or numeric methods are required to obtain the intersection of the reflectance maps[7-10]. However, the advantage is that the surface depth can be also directly calculated.

2.4 System Configuration

The configuration of this system illustrated in Fig. 1. Let the X-Y plane of the world coordinate system be perpendicular to the ground. The Z axis passes through the optical center of the lens. Four bulbs are mounted on the ring of which the center is placed on the Z axis with a distance d_1 from the origin. In addition, the ring can be rotated to adjust the light positions.

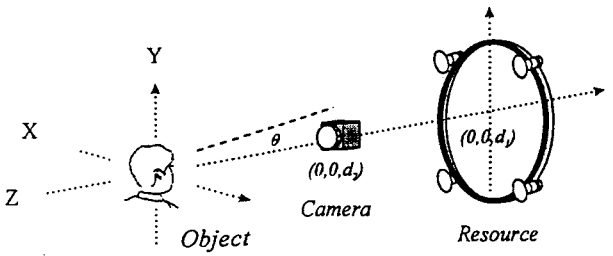

Fig. 1 System configuration

The four light bulbs are equally separated on the ring. The direction vectors of the light bulbs have a zenith angle θ. One thing that has to be compromised is to select the value of $tan\theta$. The smaller the value of $tan\theta$, the less the shadow will appear on the object. However, this also causes the light matrix **L** ill-conditioned. Emperically, the value of $tan\theta$ is chosen to be around 0.2.

The camera is placed between the ring and the origin, and distant from the origin of d_2. The selection of the value of d_2 also needs to be compromised. When the camera is close to the object, the measurement resolution increases. But usually the shadow of the camera itself is projected on the object. Hence the camera is moved as close to the object as possible so that region of interest can be fully taken larger in size. Nevertheless, the shadow of the camera would not appear in the image.

The block diagram of the system software is shown in Fig. 2. The acquired image sets are passed to the reconstruction module and the data base unit. After reconstruction, 3D data are provided to *3D Display* where both wire-frame mode and shading more are supported. The reconstructed data can also be stored in the data base for later use or other application. The file format in the data base is opened for external fetch. This increases the flexibility and extensibility.

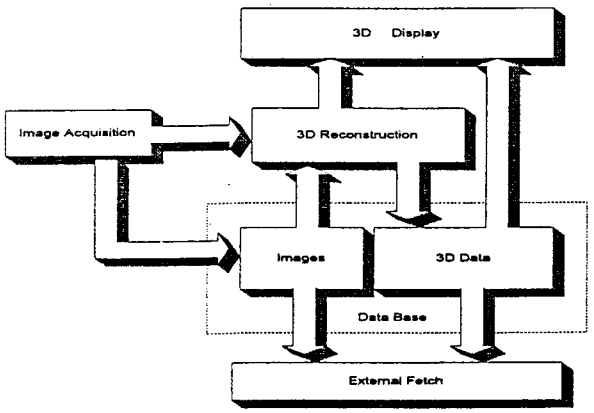

Fig. 2 The block diagram of the software design.

3. METHOD

3.1 Background Image Removal

At first, the input images are smoothed by an averaging filter of an 3x3 mask to reduce the noise caused by the camera. Since the object does not occupy the whole view, background removal is needed. A threshold selected using Otsu's method[11] is used to remove the darker parts of the images. Because the points of lower gray values represent either shadows or background, a further step is needed to separate these two kinds of areas.

The shadow appears in different areas in the images taken under different light directions. A binary template is obtained by combining the four thresholded images with logical "OR" operation. Therefore, the black areas on this binary template is considered to be the background. By comparing the template with the original images, the object and the background can be separated.

3.2 Shadow Handling

Since the radiance information is lost in shadow areas, we take the fourth image for compensation. The shadow areas should be discriminated first. Here we take the statistical approach proposed in [10].

The reflectance factor of a surface point can be estimated by Eq. (4). Under the condition that the reflection characteristics of the surface is uniform and lambertian, the reflectance factors of all surface points would be normally distributed with a small value of standard deviation. However, the shadows, inter-reflection and specularity attenuate or strengthen the radiant intensities of the surface points and thus might cause the calculated reflectance factors higher or lower than their correct values. Therefore, only those points with the reflectance factor falling in the central region of the distribution are reliable. Using these characteristics, the areas with incorrect intensities can be detected. Here we define the reliable region of the distribution of reflectance factors as twice the standard deviation over and under the mean value. In this way, not only shadows but also inter-reflection and specularity can be discriminated.

After the incorrect areas are separated, the surface points can be classified into three classes. Class I are those points which can be illuminated by all of the four light sources. The surface points illuminated by three lights and less than three are categorized as class II and class III, respectively.

Theoretically, four equations are given for each point in class I, but only one solution will be figured out. However, systematic errors make this impossible. Thus, four normals will be generated by any three of four equations and the average normal is to be selected. In addition, specular distortion can be reduced by throwing away the one farther apart from the other three.

The surface normals of class II are uniquely determined by using the algorithm as previously described. Finally, due to the information not enough for the surface points in class III, linear interpolation with determined surface orientations in the neighbor is used.

3.3 Near Point Source Model

In this study, the near point source model is employed for taking the light sources setting into account. The light direction vector varies with the position of surface point. The reflectance equation becomes

$$I = k\frac{1}{d^2}\frac{\vec{n}\cdot\vec{l}}{\|\vec{n}\|\times\|\vec{l}\|} \tag{6}$$

where

$d = \sqrt{(x-Sx)^2+(y-Sy)^2+(z-Sz)^2}$, $\vec{n} = (n_x, n_y, n_z)$, $\vec{l} = (x-Sx, y-Sy, z-Sz)$.

and hence we have four unknows (*nx ,ny, nz*) and *z* for each reflectance map. Since it's a nonlinear system with a variable of square roots in the denominator of the equation. It is difficult to solve the four unknowns by conventional numerical method. Thus we develop an iterative algorithm to find surface orientations. The flowchart is illustrated in Fig. 3.

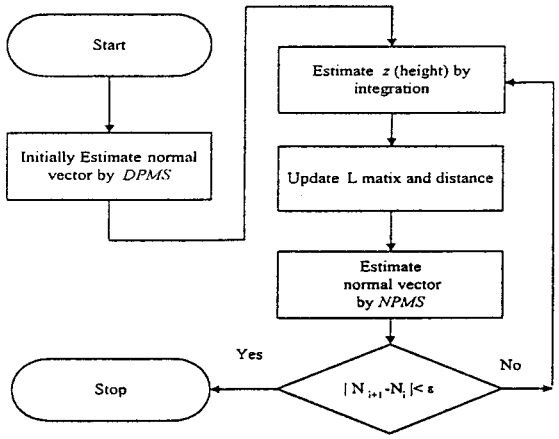

Fig. 3 The flowchart of the algorithm incorporating the near point source model.

The surface normals solved by conventional PMS (for distance point source) is used as the initial input of our algorithm. Then the height is calculated by integral method. After the four variables *nx,ny,nz* and *z* are obtained, the light direction matrix is updated and substituted into the reflectance equations for near point source model to get a new surface normal. The procedure is repeated until the difference between the current normal and the last normal is less than a defined small value of ε.

Let *i* represent the iteration number for estimation of the surface normals. Our algorithm can be summarized as follows:

STEP 1: Compute the initial normals using $n_0 = \rho \times L_0^{-1} I$.

STEP 2: Estimate the height $z_i = \iint_\Omega p_i dx + q_i dy$.

STEP 3: Update the positions of light sources as

$$L_{i+1} = \begin{bmatrix} s_{1x}-x & s_{1y}-y & s_{1z}-z_i \\ s_{2x}-x & s_{2y}-y & s_{3z}-z_i \\ s_{3x}-x & s_{3y}-y & s_{3z}-z_i \end{bmatrix}$$

STEP 4: Estimate the new normals as

$$n_{i+1} = k\frac{1}{d_{j,i+1}^2} L_{i+1}^{-1} \times I$$

STEP 5: Compute $\|n_{i+1} - n_i\| < \varepsilon$, then stop; otherwise go to STEP 2.

3.4 Height Estimation

PMS system directly gives only the surface orientations. In order to extract the shape of the object, the height value needs to be figured out. One way to reconstruct the height is to integrate the gradient[12] along a certain path (along X-axis or Y-axis) as expressed in the following equation:

$$z(x,y) = z(x_0,y_0) + \int_{(x_0,y_0)}^{(x,y)} (pdx + qdy) \tag{7}$$

where $p = \frac{\partial f(x,y)}{\partial x}, q = \frac{\partial f(x,y)}{\partial y}$.

As shown in Fig. 4, the height $Z_{(x+1,y+1)}$ can be computed by the height of previous point $Z_{(x,y+1)}$ along the X axis and $Z_{(x+1,y)}$ along the Y axis individually. Obviously, the calculated heights may not be the same value if the integration paths are different. In order to smooth the surface, average value are estimated.

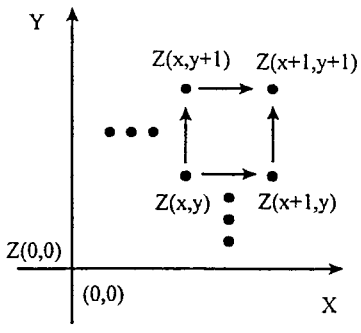

Fig. 4 The integration path

4. EXPERIMENTAL RESULTS

4.1 Lambertian Test for Human Facial Skin

The oil gland of human skin secretes sebum to prevent the skin dry and causes it to look bright and smooth. Therefore, specularity usually occurs on the human skin, especially on the face. In order to reduce the specular effect, cosmetic powder is applied to human face before the experiments is performed. The effect after using make-ups is assessed in the experimental Lambertian test for human skin.

In this experiment, two adjacent small area on the center forehead are chosen to be tested. One area is covered with the cosmetic powder and the other is not for comparison. The averaged gray values for each area are considered to be the radiance intensity of these areas.

In order to sketch the wave form of radiance variation under a fixed light source direction, the camera is moved along the semi-circle for each 7.5° from right to left and an image of the surface of forehead is acquired at each position. Therefore, 16 samples are acquired. Fig. 5 shows the experimental scheme. For every subject, the experiment is repeated three times and the data are averaged.

The results of two cases are shown in Fig. 5. In the cases of non-makeup, the gray values are going higher around the reflecting direction where specularity dominants the radiance. After using make-up, the variation of intensities abates and the standard deviation becomes smaller, and hence the specularity is reduced.

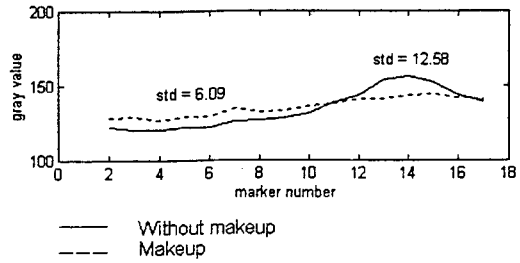

Fig. 5 The reflectance of human skin

4.2 Near Point Source Evaluation

In this research, the near point source model is employed. It is interesting to see how close the light bulbs are to the ideal point source. One way to do this is to compare the intensity distribution of an illuminated planar surface with that of simulation.

In this experiment, a piece of cardboard is fixed on the Z axis and parallel to the X-Y plane. The light bulbs is placed above the camera as close to the Z axis as possible in order to let the brightest region fall into the center of the images. 15 images are randomly acquired while the paper is rotating. After being smoothed by a median filter, 15 images are averaged to reduce the effect of inhomogeneity of reflectivity of this flat paper, and then taken for the comparison of the brightness with the theoretical values. The results are shown in Fig. 6.

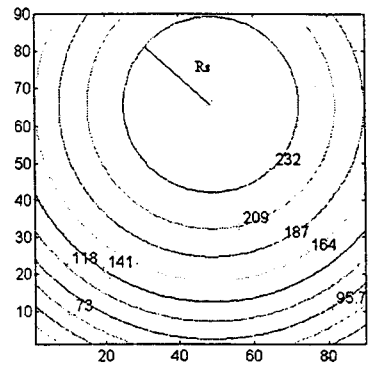

(a)

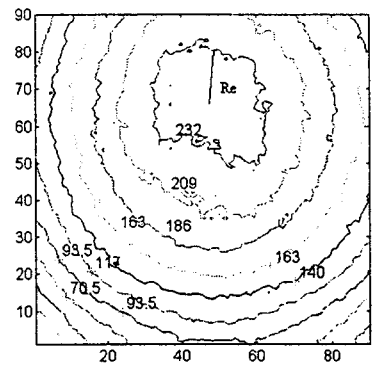

(b)

Fig. 6 The iso-brightness contours of (a) simulated and (b) real light source, respectively. These images are resized to 90X90 pixels. The brightest point of the images is considered to be the center of contours.

From Fig. 6(a), the ideal point source produces iso-brightness contours which are all concentric circles on the planar surface. In order to evaluate the similarity of the light bulb to the ideal point source, 4 parameters are defined in the following according to the intensity distribution of the simulated and experimental images.

1. The iso-brightness contours that are fitted in ellipses. The parameter R_{ab} is defined as the aspect ratios for the ratio of the minor axis to the major of the fitted ellipsoid contours. If the R_{ab} is close to 1, the characteristics of the light bulb is said to be similar to the ideal point source.
2. In the ideal case, the distance between the center and each point at iso-brightness contour on the contour R_e is supposed to be constant. The variation of R_e , R_{var} defined in Eq. (8) would be able to present this characteristics of inhomogeneity.

$$R_{\text{var}} = \frac{std(R_e)}{mean(R_e)} \tag{8}$$

3. The deviation between the simulated and experimental contours for the same intensities implies the goodness of the light source. The deviation factor R_{dev} is defined as follow:

$$R_{dev} = \sqrt{\frac{\sum_{i}^{n} \frac{|\text{Re}\,i - R_s|^2}{R_s^2}}{n}}, \tag{9}$$

where n is number of points on one contour.

4. The intensity difference between two data set is I_{dif}. It is also computed in the sense of the root mean square.

$$I_{dif} = \sqrt{\frac{\sum_{i}^{n} \frac{|I_{ei} - I_{si}|^2}{I_{si}^2}}{n}} \tag{10}$$

Finally, the four parameters are combined to give a quality factor for characterizing the performance of light bulb. The quality factor is defined as below:

$$Q = (R_{ab} + (1 - R_{dev}) + (1 - R_{\text{var}}) + (1 - I_{dif}))/4 \tag{11}$$

The quality factor for four types of light bulb as shown in Fig. 7 are evaluated. Table 1 lists the results. It is shown that the flood light has the best quality among them. Since it consumes larger power to give out stronger light beams, the S/N increases. However, it is very difficult to locate its position accurately because of its large size. Therefore, the Philips bulb is selected in our system.

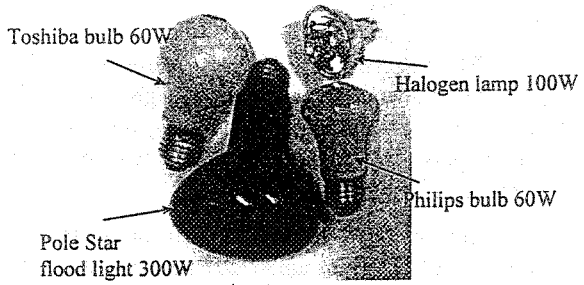

Fig. 7 Four types of light source tested in this study.

Table 1 The qualities of the light source evaluated from four proposed parameters.

	Philips bulb 60W	Halogen lamp 100W	Toshiba bulb 60W	Flood light 300W
R_{ab}	0.91	0.83	0.85	0.88
R_{dev}(%)	19.37	17.22	18.98	14.98
R_{var}(%)	8.85	10.60	10.46	7.91
I_{dif}(%)	12.53	27.57	13.72	10.61
Quality	**0.88**	**0.82**	**0.85**	**0.89**

4.3 Real Surface Reconstruction

Case 1 : Roof Surface

A roof surface made of two pieces of cardboard as shown in Fig. 8(a) is tested. Reconstructed surfaces of the conventional PMS and our method are given in Figs. 8(b). The results of conventional PMS is seriously distorted since conventional PMS assumes distant point light source. Our method improves the reconstructed shape. The improvement can be also observed from the reconstructed x-component of normal vectors as shown in Figs. 8(c). The results for y-component and z-component show the similar trend.

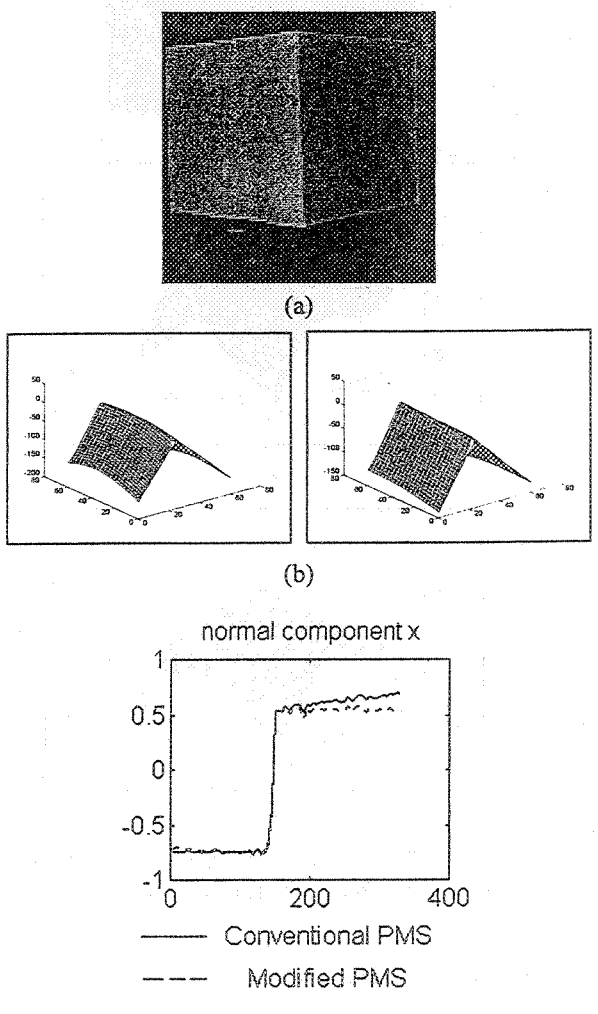

Fig. 8 (a) the original roof surface, (b) the reconstructed surface using conventional PMS(left) and our algorithm(right), and (c) the x-component of normal vectors in a cross view.

Case 2: Snow White Mask

The range data of the mask obtained from a 3D digitizer (OES-HSINCHU-3D) is used for accuracy evaluation of our system. Fig. 9(a) shows the original image. Fig. 9(b) and (c) are the whole data set for comparison. The maximum absolute error is about 4.68 mm and the mean error is about 1.54 mm. The reconstructed shape is very close to the real data. This implies the relative positions of the surface points can be accurately measured.

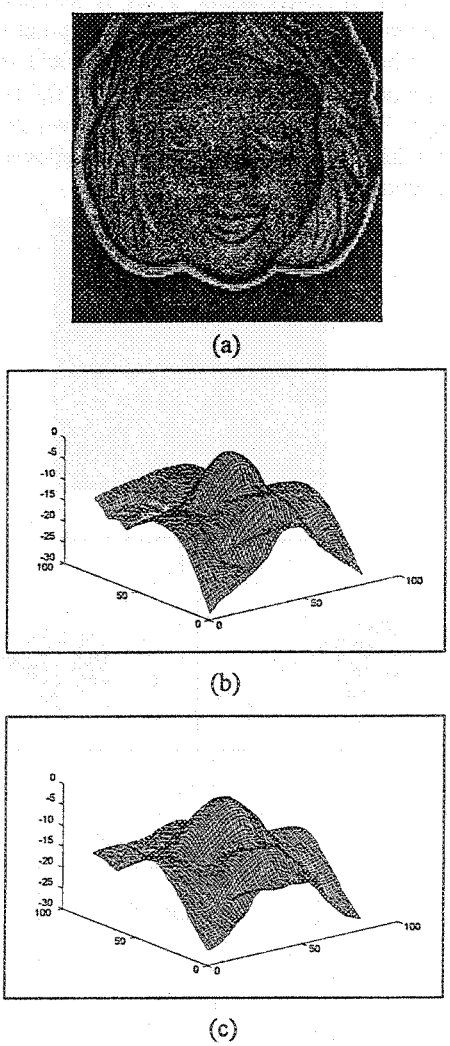

(a)

(b)

(c)

Fig. 9 (a) The Snow White mask, (b) the range data, and (c) the reconstructed data.

Case 3 : Real Human Face

Finally, a real human face is tested. The original image and the results are shown in Fig. 10. The results are not as good as expected. Because not only the shadow and discontinuity but also the inhomogenuity of the human face would also cause shape distortion. For example, the color and reflection property of the lips are different from that of facial skin.

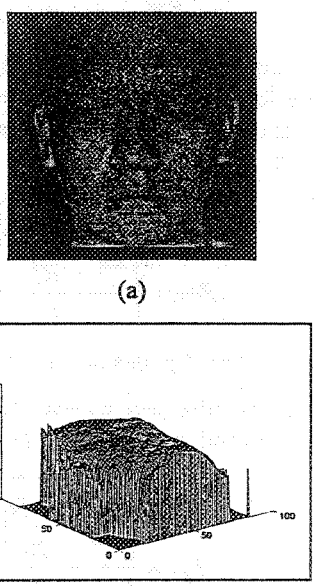

(a)

(b)

Fig. 10 (a) The real human face and (b) its reconstructed height map

5. CONCLUSIONS

In this study, a prototype PMS system is setup. This system offers the fast and convenient method for surface reconstruction. From the experimental results, it is shown that the introduction of the near point source model to PMS method improves the accuracy, and that the iterative method is demonstrated to be convergent empirically. Four images taken in our system may reduce the effect of shadows.

PMS performs well in the measurements of smooth and near lambertian surfaces. Though the surface of human face exhibits strong specularity, the application of cosmetic powder is an effective way to reduce the specular component of radiance.

Some other problems are still encountered in the application of PMS to human facial surface measurement. Firstly, in the black areas such as eye brows, nares, *etc.*, shading information is lost so that the reconstruction is failed. In addition, the discontinuous areas such as nostrils cause a serious error propagation in the integration process. Therefore, the height estimation algorithm should be modified to overcome the discontinuity.

In the future, automatic light positioning can be implemented to reduce position measurement errors. Secondly, optimal light condition for minimum shadows needs to be further investigated. Finally, this system may be extended to reconstruct the total surface contours based upon the multiple view PMS.

6. REFERENCES

[1] M. W. Vannier, T. Pilgram, G. Bhatia, and B. Brunsden, "Facial surface scanner," IEEE Comput. Graph. Appl., vol. 11, pp. 72-80, 1991.

[2] J. P. Moss, A. D. Linney, S. R. Grindrod, and C. A. Mosse, "A laser scanning system for the measurement of facial surface morphology," Opt. Lasers Eng., vol. 10, pp. 179-190, 1989.

[3] S. T. Young, S. W. Yip, H. C. Cheng, and D. B. Shieh, "Three-dimensional surface digitizer for facial contour capture," IEEE Eng. Med. Biol., vol. 13, no.1, pp. 125-141, 1994.

[4] R. J. Woodham. "Photometric method for determining surface orientation from multiple images," Opt. Eng. no. 1, pp. 139-144, 1980.

[5] J. D. Foley, A. van Dam, S. K. Feiner and J. F. Houghes, *Computer Graphics, Principles and Practice*, Addison Wesley, Reading, MA, 1990.

[6] S. Sakane, T. Sato, and M. Kakikura, "Automatic planning of light source placement for an active photometric stereo system," IEEE Int. Workshop Intell. Rob. Syst., pp. 559-566, 1990.

[7] B. Kim and P. Burger, "Calculation of surface position and orientation using the photometric stereo method," Proc. Conf. Comput. Vision and Pattern Recog., pp. 492-497, 1988.

[8] H. Kammei and S. Yamaguchi, "A method for reconstructing the shape of object from two images taken under point light source illumination," Syst. and Comput. JPN., vol. 71-D, no. 11, pp. 2319-2326, 1989.

[9] N. Kolagani and J. S. Fox, "Photometric stereo using point light sources," IEEE Int. Conf. Rob. Autom, pp. 1759-1764, 1992.

[10] C. Cho and H. Minamitani, "A new photometric method using three point light sources," IEICE Trans. Inf. Syst., vol. E76-D, no. 8, pp. 898-904, 1993.

[11] N. Otsu, "A threshold selection method from gray-level histograms," IEEE Trans. Syst., Man, Cybern., vol. SMC-9, no. 1, pp. 62-66, Jan. 1979.

[12] O. E. Vega and Y. H. Yang, "Shading logic: A heuristic approach to recover shape from shading," IEEE Trans. Pattern Anal. Mach. Intell., vol. 15, no. 6, 1993.